

Hollow Spherical Nucleic Acids for Intracellular Gene Regulation Based upon Biocompatible Silica Shells

Kaylie L. Young,^{†,‡} Alexander W. Scott,^{‡,§} Liangliang Hao,^{†,‡} Sarah E. Mirkin,^{†,‡} Guoliang Liu,^{†,‡} and Chad A. Mirkin*,^{†,‡,§}

[†]Department of Chemistry, Northwestern University, 2145 Sheridan Road, Evanston, Illinois 60208, United States

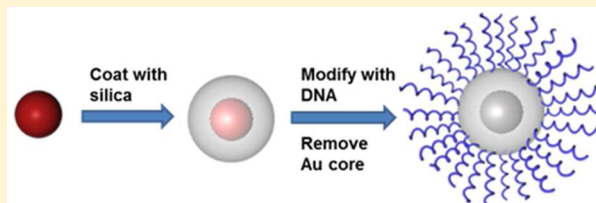
[‡]International Institute for Nanotechnology, Northwestern University, 2145 Sheridan Road, Evanston, Illinois 60208, United States

[§]Department of Biomedical Engineering, Northwestern University, 2145 Sheridan Road, Evanston, Illinois 60208, United States

S Supporting Information

ABSTRACT: Cellular transfection of nucleic acids is necessary for regulating gene expression through antisense or RNAi pathways. The development of spherical nucleic acids (SNAs, originally gold nanoparticles functionalized with synthetic oligonucleotides) has resulted in a powerful set of constructs that are able to efficiently transfect cells and regulate gene expression without the use of auxiliary cationic cocarriers. The gold core in such structures is primarily used as a template to arrange the nucleic acids into a densely packed and highly oriented form. In this work, we have developed methodology for coating the gold particle with a shell of silica, modifying the silica with a layer of oligonucleotides, and subsequently oxidatively dissolving the gold core with I₂. The resulting hollow silica-based SNAs exhibit cooperative binding behavior with respect to complementary oligonucleotides and cellular uptake properties comparable to their gold-core SNA counterparts. Importantly, they exhibit no cytotoxicity and have been used to effectively silence the eGFP gene in mouse endothelial cells through an antisense approach.

KEYWORDS: Spherical nucleic acid, oligonucleotide, silica nanoparticle, gene regulation



Recent work has shown that spherical nucleic acids (SNAs), structures consisting of linear nucleic acids that are highly oriented and densely packed on the surface of a spherical nanoparticle (NP), exhibit the ability to efficiently enter cells without a transfection agent.^{1,2} This is in contrast to free linear nucleic acids, which generally require a cationic moiety to neutralize their negative charge to pass through the cellular membrane.³ However, these cationic lipids and polymers often display cytotoxic effects at high concentrations and the inability to be degraded biologically.^{4–6} SNA-NP conjugates thus provide a unique platform for internalizing large quantities of nucleic acids into cells under mild conditions that can subsequently be used for intracellular detection⁷ and gene regulation.¹ Thus far, we have shown that scavenger receptors mediate the cellular entry of SNAs⁸ and cellular uptake is dependent on the density of nucleic acids on the nanoparticle surface.⁹ Furthermore, SNA-NP conjugates have a unique set of properties that are advantageous for intracellular applications, including high binding coefficients for DNA that is complementary and RNA,¹⁰ nuclease resistance,¹¹ and minimal immune response.¹² With respect to cellular internalization and activity, these observations are all based upon the hypothesis that the unique properties of the SNA architecture stem from the oligonucleotide shell and the density and orientation of the nucleic acids that comprise it as opposed to the nanoparticle core. Importantly, we recently demonstrated a synthetic route for making hollow SNAs by cross-linking oligonucleotides on

the surface of gold nanoparticles and subsequently dissolving the gold particle template. Consistent with our hypothesis, these structures are capable of cellular internalization and gene regulation via antisense and RNAi pathways.¹³ The hollow structures are attractive, especially if one is concerned about the long-term toxicity of the gold nanoparticle core.^{14–16} The disadvantage of the approach is that specialty oligonucleotides capable of cross-linking are required, and at present, they are prohibitively expensive. These observations pose the challenge of identifying other chemical routes to hollow SNA structures that possess similar properties to those derived from gold particles and perhaps offer even greater capabilities.

Herein we report a new class of core-free SNA conjugate consisting of a biocompatible porous silica shell. By using a silica-coated gold nanoparticle as a template, we can easily functionalize it with nucleic acids using a wide variety of coupling strategies and relatively simple and readily available coupling molecules. Significantly, the silica shell acts as a cross-linked scaffold to assemble oriented oligonucleotides with a porous architecture that allows one to chemically dissolve the gold core. The hollow silica SNAs maintain the unique properties of the SNA gold nanoparticle conjugates^{2,7–13,17} and exhibit the ability to be internalized by cells without a

Received: June 1, 2012

Revised: June 19, 2012

Published: June 22, 2012

transfection agent and efficiently knock down a target mRNA sequence. Moreover, silica is an attractive material from a biological perspective since it is known to degrade into bioinert silicic acid under physiological conditions.¹⁸ Previous studies of porous silica nanoparticles have shown a degradation rate of approximately 15% per day in a cellular environment.¹⁹ In principle, these new SNA conjugates should degrade over time and release active oligonucleotides.

To prepare the silica (SiO_2) shells, 13 nm citrate-stabilized gold nanoparticles (Au NP) were synthesized to serve as sacrificial templates.^{20,21} The Au NPs were passivated with a short poly(ethylene glycol) (PEG) chain containing a thiol functional group on one end and a carboxylic acid on the other ($\text{SH}-(\text{CH}_2)_{11}-\text{(EG)}_6-\text{OCH}_2-\text{COOH}$) and redispersed in ethanol. The Au NPs were directly coated with a thin layer (~15 nm) of silica using an ammonia-catalyzed hydrolysis of tetraethyl orthosilicate (TEOS) and subsequent condensation of silicic acid to give a network of tetrahedral SiO_4 units with shared vertices.²² The thickness of the silica shell can easily be controlled by changing the relative concentrations of Au NPs, water, ammonia, and silicon alkoxide in the reaction.²³ The resulting Au core-silica shell (Au@SiO_2) particles were heated at 60 °C for 24 h to ensure a homogeneous silica shell (see experimental details in the Supporting Information).²⁴

To achieve a dense layer of DNA on the silica shell surface, the heterobifunctional cross-linker *p*-maleimidophenyl isocyanate (PMPI) was used since cross-linkers with amine-reactive isocyanates have demonstrated improved retention of maleimide activity compared with NHS-ester based linkers.²⁵ The Au@SiO_2 NPs were first derivatized with (aminopropyl)-triethoxysilane (APTES) and subsequently activated with amine-reactive PMPI to introduce thiol-reactive maleimide groups.²⁵ The addition of DNA oligonucleotides designed to target an mRNA sequence coding for enhanced green fluorescent protein (eGFP) with terminal propylthiol groups (3'SH(C_3H_6)-AAAAAAAAAGGTGTTCAAGTCGCA-CAGGC5'), followed by the slow addition of NaCl to 0.3 M, led to the formation of polyvalent Au@SiO_2 particles with a loading of ~75 strands per particle. Upon selective oxidative dissolution of the Au NP core with I_2 , hollow SiO_2 SNAs are formed (Figure 1). Finally, the silica SNAs were dialyzed overnight against water to remove I_2 remaining in solution.

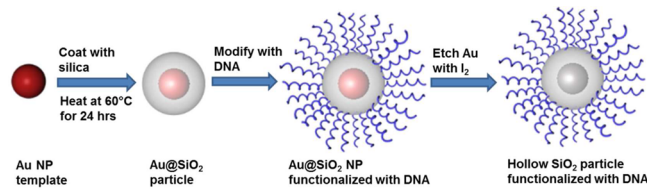


Figure 1. Synthesis of DNA functionalized hollow SiO_2 particles using gold nanoparticles as sacrificial templates.

The ability of I_2 to oxidatively dissolve the gold core indicates that the silica shells remain porous through the heating and DNA functionalization steps. The Au@SiO_2 and gold-free SiO_2 particles were characterized by scanning transmission electron microscopy (STEM) in scanning, z -contrast, and transmission modes (Figure 2A–C and D–F, respectively). Indeed, the microscopy images indicate that the Au NP cores are entirely dissolved upon the addition of I_2 and a hollow interior remains. Importantly, the silica shells remain as discrete particles and maintain their structure upon dissolution of the gold core, a

conclusion also verified by dynamic light scattering (DLS). Initially the Au NPs had an average hydrodynamic radius of 17.3 ± 0.8 nm. After the deposition of the silica shells onto the Au NP templates, this value increased to 47.7 ± 10.1 nm. Upon functionalization with DNA using APTES and PMPI, the final hydrodynamic radius was measured to be 85.8 ± 16.4 nm. It should be noted that the DLS measurements of the hydrated particles are slightly larger than the diameters of the dry particles measured with electron microscopy.²⁶ However, the trend in the DLS data is indicative of growth at each step in the synthesis without the formation of large aggregates. The synthesis of the silica SNAs was also monitored with UV-vis spectroscopy (Figure 3A). The UV-vis spectra reveal that the Au@SiO_2 particles exhibit a distinct absorption at ~ 530 nm that is characteristic of dispersed gold nanoparticles albeit slightly red-shifted compared to Au NPs due to the increase in the dielectric constant of the silica shell.^{27–29} After the addition of I_2 , the absorption band at 530 nm is no longer present, consistent with the removal of the Au core.

Previously, we have shown that SNAs, when hybridized with complementary oligonucleotides, exhibit narrow melting transitions compared with free DNA strands due to a high degree of cooperative binding.³⁰ This phenomenon is also observed for hollow SNAs consisting of cross-linked nucleic acids.¹³ Due to the layer of highly oriented oligonucleotides on the surface of the silica shells (~75 DNA strands per particle when salted to 0.3 M NaCl, determined by the OliGreen Assay), it was hypothesized that both the Au@SiO_2 particles and the hollow silica SNAs would exhibit cooperative binding behavior as well. Upon the addition of a self-complementary linker strand that binds to the oligonucleotides on the silica surface, the particles formed visible aggregates, which were then dehybridized by slowly increasing the temperature. As shown in Figure 3B, the aggregated SiO_2 particles exhibit a sharp melting transition (fwhm of the derivative = ~ 2 °C), indicative of cooperative behavior.²

Once it was confirmed that the Au@SiO_2 and core-free SiO_2 SNAs retain the cooperative binding properties of Au NPs densely functionalized with nucleic acids, the ability of these particles to be transfected into cells and facilitate gene regulation via the antisense pathway was investigated. To qualitatively access the cellular uptake of the SiO_2 SNAs, particles with and without the Au NP core were functionalized with Cy5 dye-labeled anti-eGFP DNA oligonucleotides. The particles (5 nM) were then incubated overnight with C166 mouse endothelial cells stably expressing the eGFP gene. It is important to note that no cationic transfection agent was included during the incubation step. The C166 cells were washed, fixed, and imaged by laser scanning confocal microscopy. As shown in Figure 4A, both the Au@SiO_2 and the hollow SiO_2 particles are taken into the cytoplasm of the C166 cells. The mechanism of cellular uptake of SNAs has previously been demonstrated to involve receptor-mediated endocytosis⁸ and stems from the dense, highly oriented layer of nucleic acids.² It is therefore hypothesized that a similar mechanism applies for the DNA functionalized Au@SiO_2 and hollow SiO_2 particles. Note that neither of these particles enter the nuclei of the cells because of their size. Images of planes collected at various depths within the cell samples (z -stack) further confirmed cellular uptake (see the Supporting Information).

The silica-based SNAs were next evaluated for their ability to regulate target genes. Au@SiO_2 particles, hollow SiO_2 particles,

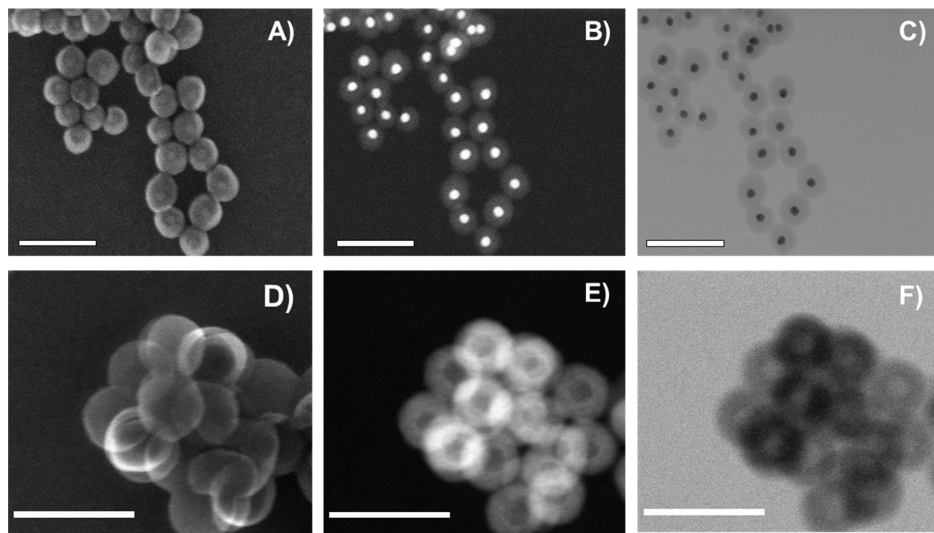


Figure 2. STEM images of Au@SiO₂ particles (A–C) and hollow SiO₂ particles (D–F) in scanning, z-contrast, and transmission modes, respectively. In A–C, the Au NP cores are visible. After the addition of I₂, the Au NP cores dissolve leaving a hollow interior (E–F). Scale bars are 100 nm.

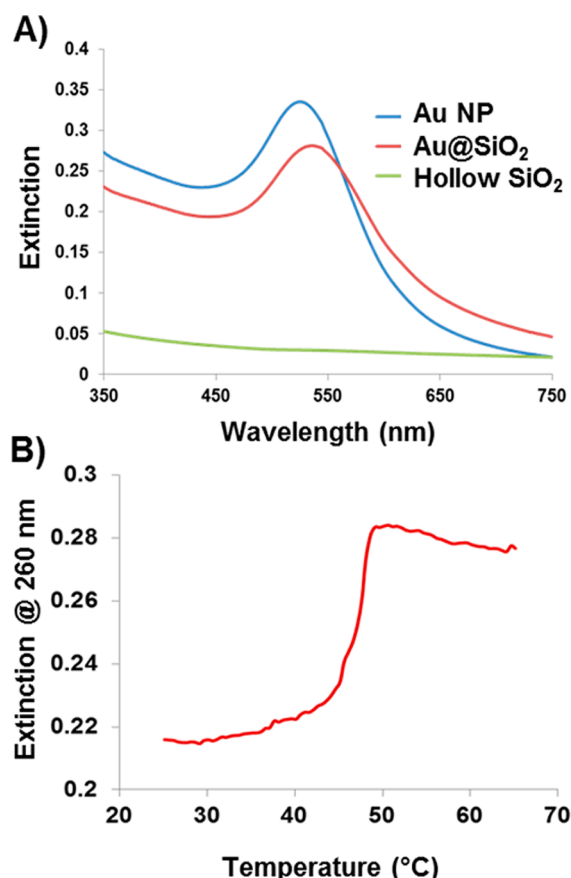


Figure 3. (A) Extinction spectra of Au NP templates, silica-coated Au NPs (Au@SiO₂), and hollow SiO₂ particles resulting from the treatment of the Au@SiO₂ particles with I₂. The Au@SiO₂ particles exhibit a distinct absorption at ~530 nm that is characteristic of Au NP, albeit slightly red-shifted due to the silica shell. After treatment with I₂, the hollow SiO₂ particles do not contain this absorption band, confirming the dissolution of the Au NP core. (B) Melting analysis of DNA functionalized SiO₂ particles hybridized using a self-complementary linker. The sharp melting transition (full-width half-max = ~2 °C) is indicative of cooperative binding.

and Au NPs were functionalized with anti-eGFP DNA oligonucleotides and incubated (5 nM) with C166 cells stably expressing eGFP. Particles functionalized with nontargeting scrambled DNA oligonucleotides served as a negative control. The cells were then collected, lysed, and analyzed for their eGFP mRNA levels by quantitative real-time reverse transcriptase polymerase chain reaction (qRT-PCR). mRNA levels of cells treated with anti-eGFP Au@SiO₂ particles and core-free SiO₂ shells were significantly reduced by 68% and 50%, respectively, when compared with those treated with scrambled “nonsense” DNA particles (Figure 4B). Importantly, the amount of knockdown is comparable to that observed with DNA functionalized Au NPs (~52%). Furthermore, the Au@SiO₂ particles and hollow SiO₂ SNAs were shown to exhibit low cytotoxicity toward C166 cells using the 3-(4,5-dimethylthiazol-2-yl)-2,5-diphenyl tetrazolium bromide (MTT) assay. As indicated in Figure 4C, cells treated with the targeted and nontargeted DNA oligonucleotides for 8 h showed up to 95% viability compared with a nontreated control. Taken together, these data suggest that this new class of core-free SNA retains the unique properties of the Au NP SNAs, including efficient cellular uptake without the need for conventional cationic transfection agents, a high capacity for gene regulation, and low cytotoxicity.

The present work describes a simple, scalable, and biocompatible SNA construct that serves to confirm our hypothesis that the emergent properties of SNAs are a result of the layer of oriented oligonucleotides and not the inorganic nanoparticle core. The use of silica as the cross-linking reagent makes this construct extremely versatile; the thickness and porosity of the silica shell is tunable with reaction conditions, and many well-established coupling chemistries including EDC/NHS-ester,³¹ copper-catalyzed³² or copper-free³³ click chemistry, and reductive amination³⁴ can be utilized to achieve a densely packed, oriented nucleic acid shell. Additionally, there are potential benefits of a hollow architecture including tunable degradation profiles and the ability to load the hollow interior with biologically relevant molecules or drugs. Indeed, these novel core-free SiO₂ SNAs represent a new class of SNA that shows promise for a wide range of intracellular gene regulation.

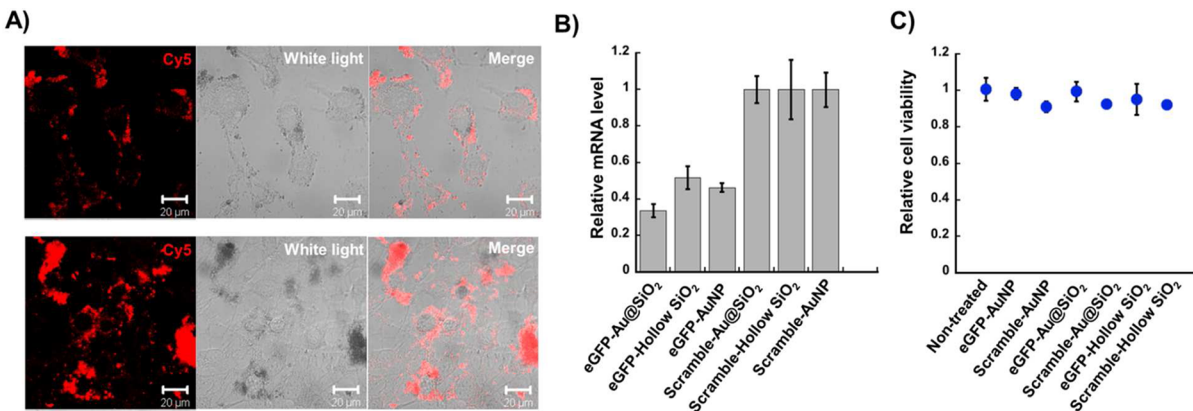


Figure 4. Cellular uptake and response of the DNA functionalized Au@SiO₂ and hollow SiO₂ particles in C166 cells. (A) C166 cells were treated with Au@SiO₂ particles (upper panel) and hollow SiO₂ particles (lower panel) functionalized with Cy5 dye-labeled anti-eGFP DNA oligonucleotides. Cy5 fluorescence is observed in the cytoplasm, but not in the nuclei, indicating the internalization of the particles into the cells. Scale bars are 20 μm. (B) eGFP knockdown at the mRNA level determined by qRT-PCR. mRNA levels of cells treated with anti-eGFP DNA oligonucleotide functionalized Au@SiO₂ and hollow SiO₂ particles were significantly reduced when compared with those treated with scrambled-sequence DNA particles. (C) Minimal cell toxicity of the Au@SiO₂ and hollow SiO₂ particles toward C166 cells was detected using the MTT assay. Cells treated with the eGFP-targeted and nontargeted DNA oligonucleotides showed up to 95% viability compared with nontreated cells.

applications and, therefore, constitutes a new class of nanotherapeutics.

■ ASSOCIATED CONTENT

Supporting Information

Experimental procedures and z-stack of incubated cells (Figure S1). This material is available free of charge via the Internet at <http://pubs.acs.org>.

■ AUTHOR INFORMATION

Corresponding Author

*E-mail: chadnano@northwestern.edu. Tel.: (847) 467-7302.

Notes

The authors declare no competing financial interest.

■ ACKNOWLEDGMENTS

C.A.M. acknowledges support from AFOSR Award FA9550-11-1-0275, NSSEFF Awards N00244-09-1-0012 and N00244-09-1-0071, CCNE initiative of NIH Awards U54 CA119341 and U54 CA151880, Dixon Translational Research Grants Initiative, NSEC initiative of NSF Award EEC-0647560, Prostate Cancer Foundation, NIAMS/NIH grants R01AR060810 and R21AR062898, and DARPA/MTO Award N66001-11-1-4189. K.L.Y. acknowledges the National Science Foundation and the National Defense Science and Engineering Graduate Research Fellowships. A.W.S. acknowledges CCNE initiative of supplemental NCI/NIH Award 3U54CA151880. The content is solely the responsibility of the authors and does not necessarily represent the official views of the sponsor organizations. K.L.Y., A.W.S., L.H., S.E.M., G.L., and C.A.M. designed and performed experiments. K.L.Y., A.W.S., L.H., and C.A.M. wrote the manuscript.

■ REFERENCES

- (1) Rosi, N. L.; Giljohann, D. A.; Thaxton, C. S.; Lytton-Jean, A. K. R.; Han, M. S.; Mirkin, C. A. *Science* **2006**, *312*, 1027–1030.
- (2) Cutler, J. I.; Auyeung, E.; Mirkin, C. A. *J. Am. Chem. Soc.* **2012**, *134*, 1376–1391.
- (3) Sokolova, V.; Epple, M. *Angew. Chem., Int. Ed.* **2008**, *47*, 1382–1395.
- (4) Lv, H.; Zhang, S.; Wang, B.; Cui, S.; Yan, J. *J. Controlled Release* **2006**, *114*, 100–109.
- (5) Dokka, S.; Toledo, D.; Shi, X.; Castranova, V.; Rojanasakul, Y. *Pharm. Res.* **2000**, *17*, 521–525.
- (6) Soenen, S. J. H.; Brisson, A. R.; De Cuyper, M. *Biomaterials* **2009**, *30*, 3691–3701.
- (7) Seferos, D. S.; Giljohann, D. A.; Hill, H. D.; Prigodich, A. E.; Mirkin, C. A. *J. Am. Chem. Soc.* **2007**, *129*, 15477–15479.
- (8) Patel, P. C.; Giljohann, D. A.; Daniel, W. L.; Zheng, D.; Prigodich, A. E.; Mirkin, C. A. *Bioconjugate Chem.* **2010**, *21*, 2250–2256.
- (9) Giljohann, D. A.; Seferos, D. S.; Patel, P. C.; Millstone, J. E.; Rosi, N. L.; Mirkin, C. A. *Nano Lett.* **2007**, *7*, 3818–3821.
- (10) Lytton-Jean, A. K. R.; Mirkin, C. A. *J. Am. Chem. Soc.* **2005**, *127*, 12754–12755.
- (11) Seferos, D. S.; Prigodich, A. E.; Giljohann, D. A.; Patel, P. C.; Mirkin, C. A. *Nano Lett.* **2009**, *9*, 308–311.
- (12) Massich, M. D.; Giljohann, D. A.; Seferos, D. S.; Ludlow, L. E.; Horvath, C. M.; Mirkin, C. A. *Mol. Pharmaceutics* **2009**, *6*, 1934–1940.
- (13) Cutler, J. I.; Zhang, K.; Zheng, D.; Auyeung, E.; Prigodich, A. E.; Mirkin, C. A. *J. Am. Chem. Soc.* **2011**, *133*, 9254–9257.
- (14) Bhabra, G.; Sood, A.; Fisher, B.; Cartwright, L.; Saunders, M.; Evans, W. H.; Surprenant, A.; Lopez-Castejon, G.; Mann, S.; Davis, S. A.; Hails, L. A.; Ingham, E.; Verkade, P.; Lane, J.; Heesom, K.; Newson, R.; Case, C. P. *Nat. Nanotechnol.* **2009**, *4*, 876–883.
- (15) Nel, A.; Xia, T.; Maedler, L.; Li, N. *Science* **2006**, *311*, 622–627.
- (16) Chompooosor, A.; Saha, K.; Ghosh, P. S.; Macarthy, D. J.; Miranda, O. R.; Zhu, Z.-J.; Arcaro, K. F.; Rotello, V. M. *Small* **2010**, *6*, 2246–2249.
- (17) Letsinger, R. L.; Elghanian, R.; Viswanadham, G.; Mirkin, C. A. *Bioconjugate Chem.* **2000**, *11*, 289–291.
- (18) Park, J.-H.; Gu, L.; von Maltzahn, G.; Ruoslahti, E.; Bhatia, S. N.; Sailor, M. J. *Nat. Mater.* **2009**, *8*, 331–336.
- (19) Yamada, H.; Urata, C.; Aoyama, Y.; Osada, S.; Yamauchi, Y.; Kuroda, K. *Chem. Mater.* **2012**, *24*, 1462–1471.
- (20) Frens, G. *Nat. Phys. Sci.* **1973**, *241*, 20–22.
- (21) Marinakos, S. M.; Novak, J. P.; Brousseau, L. C., III; House, A. B.; Edeki, E. M.; Feldhaus, J. C.; Feldheim, D. L. *J. Am. Chem. Soc.* **1999**, *121*, 8518–8522.
- (22) Lu, Y.; Yin, Y.; Li, Z.-Y.; Xia, Y. *Nano Lett.* **2002**, *2*, 785–788.
- (23) Mine, E.; Yamada, A.; Kobayashi, Y.; Konno, M.; Liz-Marzan, L. M. *J. Colloid Interface Sci.* **2003**, *264*, 385–390.
- (24) Wong, Y. J.; Zhu, L.; Teo, W. S.; Tan, Y. W.; Yang, Y.; Wang, C.; Chen, H. *J. Am. Chem. Soc.* **2011**, *133*, 11422–11425.
- (25) Jin, L.; Horgan, A.; Levicky, R. *Langmuir* **2003**, *19*, 6968–6975.

- (26) Barnes, C. A.; Elsaesser, A.; Arkusz, J.; Smok, A.; Palus, J.; Lesniak, A.; Salvati, A.; Hanrahan, J. P.; de Jong, W. H.; Dziubaltowska, E.; Stepnik, M.; Rydzynski, K.; McKerr, G.; Lynch, I.; Dawson, K. A.; Howard, C. V. *Nano Lett.* **2008**, *8*, 3069–3074.
- (27) Xue, C.; Chen, X.; Hurst, S. J.; Mirkin, C. A. *Adv. Mater.* **2007**, *19*, 4071–4074.
- (28) Banholzer, M. J.; Harris, N.; Millstone, J. E.; Schatz, G. C.; Mirkin, C. A. *J. Phys. Chem. C* **2010**, *114*, 7521–7526.
- (29) Kelly, K. L.; Coronado, E.; Zhao, L. L.; Schatz, G. C. *J. Phys. Chem. B* **2003**, *107*, 668–677.
- (30) Jin, R.; Wu, G.; Li, Z.; Mirkin, C. A.; Schatz, G. C. *J. Am. Chem. Soc.* **2003**, *125*, 1643–1654.
- (31) Hermanson, G. T. *Bioconjugate Techniques*, 2nd ed.; Academic Press: San Diego, CA, 2008.
- (32) Kolb, H. C.; Finn, M. G.; Sharpless, K. B. *Angew. Chem., Int. Ed.* **2001**, *40*, 2004–2021.
- (33) Baskin, J. M.; Prescher, J. A.; Laughlin, S. T.; Agard, N. J.; Chang, P. V.; Miller, I. A.; Lo, A.; Codelli, J. A.; Bertozzi, C. R. *Proc. Natl. Acad. Sci. U.S.A.* **2007**, *104*, 16793–16797.
- (34) Liu, S.; Han, M. *Adv. Funct. Mater.* **2005**, *15*, 961–967.